The 30–60-Day Convection Seesaw between the Tropical Indian and Western Pacific Oceans*

BAOZHEN ZHU** AND BIN WANG

Department of Meteorology, School of Ocean and Earth Science and Technology, University of Hawaii, Honolulu, Hawaii

(Manuscript received 5 December 1990, in final form 28 February 1992)

ABSTRACT

The tropical Indian and western Pacific oceans are two prominent action centers for tropical 30–60-day convective variability. When convection is enhanced over the equatorial Indian Ocean, the tropical western Pacific often experiences an abnormal dry condition (phase I), whereas the development of the convection over the tropical western Pacific tends to be accompanied by suppressed convection in the equatorial Indian Ocean (phase II). This convection seesaw is a fundamental characteristic of the tropical 30–60-day oscillation.

The seesaw is intimately associated with the activity of propagating low-frequency convective systems (LFCSs). Its formation process is season dependent. Typical boreal summer seesaw results from a time-lagged development of two systems: a western system that originates in the equatorial Indian Ocean and moves eastward and/or northward and an eastern system that develops in the western Pacific monsoon region and moves westward and/or northward. The boreal winter seesaw, on the other hand, is caused by the longitudinal dependence of the evolution of eastward-moving LFCSs that strongly amplify in the equatorial Indian Ocean, weaken and/or split when rapidly passing over the maritime continent, and reintensify in the South Pacific convergence zone (SPCZ).

There are two phases of the seesaw. During the first phase, the LFCSs interact with the Indian monsoon in boreal summer and Indonesian–Australian monsoon in boreal winter. Likewise, during the second phase, the LFCSs interplay with monsoon circulations over the western Pacific monsoon trough in boreal summer and over the SPCZ in boreal winter. The convection seesaw activity is closely tied to the corresponding active-break monsoon cycles over the two polar regions of the seesaw.

1. Introduction

The tropical 40–50-day oscillation (also known as 30–60-day oscillation) first discovered by Madden and Julian (1971) using spectral analysis of station pressure and upper-air data was interpreted as resulting from planetary-scale overturning cells moving eastward around the globe in the tropospheric equatorial plane (Madden and Julian 1972).

Lorenc (1984) and Krishnamurti et al. (1985) confirmed the existence of this planetary-scale wave by analysis of velocity potential and wind fields of 1979. Knutson and Weickmann (1987) carried out an empirical orthogonal function (EOF) analysis of 30–60-day filtered divergent and rotational winds and outgoing longwave radiation (OLR) anomalies, and obtained coherent principal patterns of eastward-propagating divergent and rotational waves in association with anomalous convective activity. Rui and Wang (1990) documented the development characteristics and dynamic structure of the 30–60-day convection anomalies by compositing 36 individual eastward-moving events, and proposed a longitude-dependent life cycle: initiation, intensification, maturity, and dissipation/emanation.

The waves associated with the 30–60-day oscillation do not always move eastward along the equator. Yasunari (1979, 1980) revealed a northward propagation of the cloudiness in the Indian monsoon region on a 30–40-day time scale. The northward-moving cloud bands are accompanied by northward migration of low-level monsoon troughs (Krishnamurti and Subrahmanyam 1982). This phenomenon was postulated as a regional component of the global eastward propagation (e.g., Julian and Madden 1981). Recently, however, it was found that only about one-half of the cases of northward propagation over the Indian Ocean and western Pacific summer monsoon regions are associated with the equatorial eastward-moving systems, the other half are not related to any eastward propagation (Wang and Rui 1990a). During boreal winter, the equatorial eastward propagation dominates, whereas during boreal summer the northward propa-

* School of Ocean and Earth Science and Technology Contribution Number 3020.

** On leave from the Institute of Atmospheric Physics, Academia Sinica, Beijing, People's Republic of China.

Corresponding author address: Dr. Bin Wang, Dept. of Meteorology, School of Ocean and Earth Science and Technology, University of Hawaii, 21525 Correa Rd., Honolulu, HI 96822.

gation in the Indian and western Pacific monsoon regions along with westward propagation in the western Pacific off-equatorial region are more active.

Another interesting feature of the tropical 30–60-day oscillation noticed by Lau and Chan (1985, 1986) is an out-of-phase relationship between the convection anomalies over the maritime continent and the central Pacific. Similar out-of-phase dipole variations exist between the Indian Ocean and the western Pacific. They have named this dipole pattern a seesaw and interpreted it, on the basis of a correlation map analysis, as resulting from systematic eastward propagation of equatorial waves. Krishnamurti et al. (1985), on the other hand, speculated that the low-frequency pressure systems associated with the convection anomalies may form elsewhere and migrate to low latitudes.

The present study is devoted to an observational analysis of 30–60-day seesaw in convection, trying to address the following questions: What is the nature of the convection seesaw between the Indian Ocean and western-central Pacific? How is it formed? How is it related to various types of propagating waves? How does the seesaw connect with monsoon circulations? We will investigate the behavior of the convection seesaw in terms of a synoptic approach—that is, by examining individual seesaw events case by case.

2. Data

The data used in this study include five years (1 November 1980–31 October 1985) of OLR data from NOAA polar orbit satellite observations and 200- and 850-mb analyzed wind data from the European Centre for Medium-Range Weather Forecasts (ECMWF). The data domain covers the global tropics and subtropics between 40°S and 40°N.

The normal annual cycle was first removed from original daily data by subtracting out the annual mean and first three Fourier harmonics of the climatological daily means. The interannual variation was further eliminated by subtracting corresponding three-month running mean anomalies from daily anomaly series. The nonoverlapping five-day averages were then computed to obtain pentad mean anomalies (PMAs), which depict intraseasonal fluctuations. In the present study, the PMA maps are the basic tools used to diagnose and synthesize the low-frequency variabilities. The detailed procedures of making PMA maps may be found in Wang and Rui (1990a).

In addition to the 200- and 850-mb wind anomalies, velocity potential χ is also computed using the Poisson equation, $-\nabla^2\chi = D$, by assuming χ vanishes at 45°N and 45°S, where D is divergence expressed in spherical coordinates. The values between 30°N and 30°S are not appreciably affected by the boundary conditions. A positive 200-mb velocity potential anomaly indicates anomalous divergence.

3. The 30–60-day convection seesaw phenomenon

a. Preferred locations of strong convection anomalies

On PMA OLR maps, a pentad mean convection anomaly (for simplicity, hereafter it will be referred to as convection anomaly) is defined by a negative OLR anomaly whose central value is lower than -15 W m^{-2} and whose zonal dimension (the zonal diameter of the area enclosed by -5 W m^{-2} contour) is larger than 30° longitude. A strong convection anomaly (SCA) is defined as a convection anomaly with a minimum OLR anomaly below -25 W m^{-2}. Based upon five-years of PMA maps of OLR, all SCA centers are stratified by season and plotted in Fig. 1.

During boreal summer (defined as the period from 1 May to 31 October) the SCA centers are biased to the Northern Hemisphere and densely populate two sectors separated by a region of suppressed variability extending from the maritime continent to the west coast of the Indo-China peninsula (Fig. 1a). The western sector covers the equatorial Indian Ocean–southern India, while the eastern sector is centered over the Philippine Sea around 140°E and 15°N. In addition, a secondary region of occurrence of SCA centers is located around central America.

During boreal winter (defined as the period from 1 November to 30 April) the majority of SCA centers lie south of the equator and are concentrated in two separate zones (Fig. 1b). The western zone extends from Madagascar first northeastward to the central equatorial Indian Ocean then southeastward into central Australia, while the eastern zone extends from the Philippine Sea southeastward all the way to the central South Pacific (140°W, 17°S). The former covers the Southwest Indian Ocean convergence zone (SWICZ), whereas the later largely coincides with the South Pacific convergence zone (SPCZ). It is of interest to notice the low density of SCA centers between the two enhanced convection zones. This low-variability zone extends from west of Sumatra to south of New Guinea. Other features include an east–west oriented region of widespread SCA centers north of the intertropical convergence zone (ITCZ) in the North Pacific and North Atlantic and a group of SCA centers over eastern South America.

There are two energy peaks with periods of 10–20 and 30–60 days, respectively, in the low-frequency variation of convection during northern summer (Yasunari 1979). Both are reflected in Fig. 1a. The distribution of SCA centers described above are generally consistent with the geographic distribution of the total variance (10–180 days) reported by Weickmann et al. (1985) and Knutson et al. (1986). In their synoptic climatology study, Wang and Rui (1990a) found that the Maritime Continent is one of the major dissipative regions, whereas the equatorial Indian Ocean and the western Pacific convergence zones (the monsoon

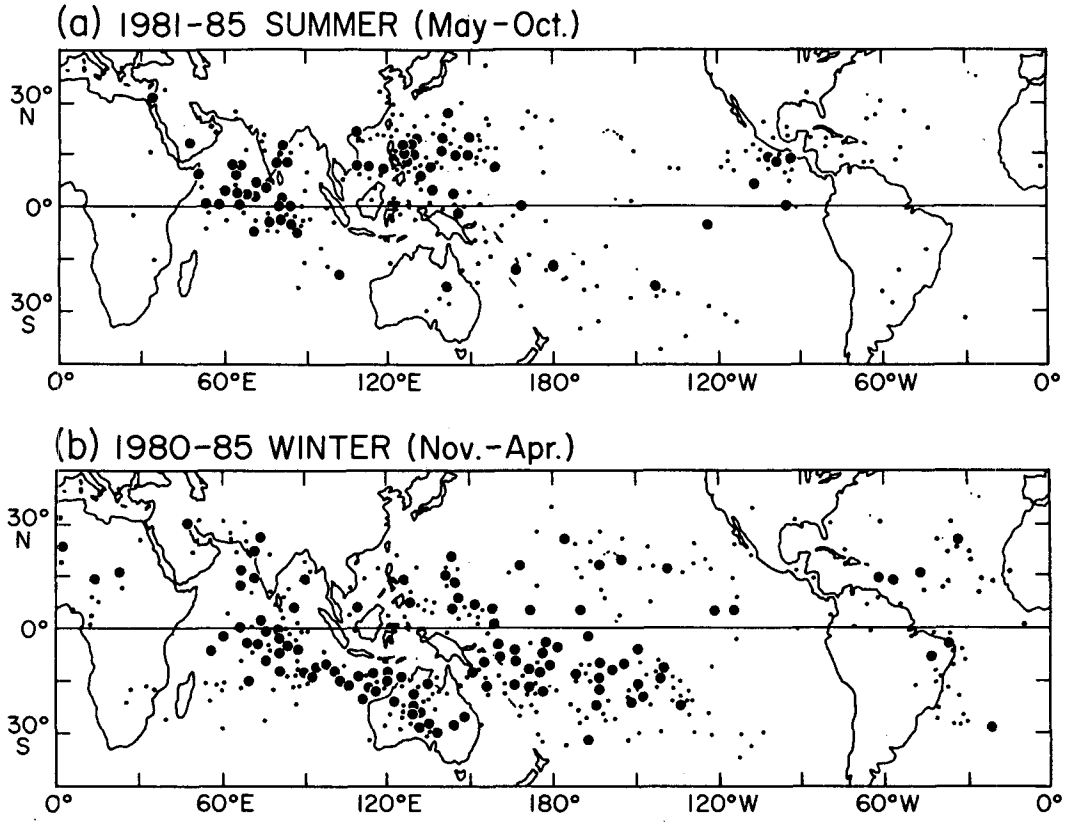

FIG. 1. Geographic distribution of the centers of strong convection anomalies appearing on 5-years' pentad mean anomaly maps for (a) May–October season and (b) November–April season. The small- and large-size dots denote centers with minimum OLR between −25 and −35 W m^{-2} and lower than −35 W m^{-2}, respectively.

trough and SPCZ) are preferred locations for the development of eastward-moving convective anomalies. The results of Fig. 1 confirm their findings in a broader perspective.

It is evident that the major regions of SCA are located in the eastern hemisphere. The seasonal march of the preferred regions of SCA is closely linked to the Northern and Southern hemisphere summer monsoons. This implies a significant influence of the monsoon circulations on 30–60-day convective activity. Comparison of the numbers of very strong convection anomaly centers (large dots) in Figs. 1a (N = 61) and 1b (N = 111), on the other hand, shows that their frequency of occurrence is substantially higher in southern summer than in northern summer, albeit the Southern Hemisphere summer monsoon is weaker than its Northern Hemisphere counterpart. This cannot be explained by the influence of the monsoons. In fact, over the Indian Ocean the majority of SCA centers occur on the periphery or outside of heavy monsoonal rain domains and are primarily scattered over the equatorial Indian Ocean. These may be of moist equatorial Kelvin wave origin. It was demonstrated that the combined dynamic (trapping) effect of the equator and the thermodynamic effect of underlying sea surface temperature (SST) control, to a large extent, the development of 30–60-day convective disturbances (Wang and Rui 1990b). When the thermal equator (defined as the latitude where SST is maximum) nearly coincides with the geographic equator as the situation in the Indian Ocean, the amplification of 30–60-day convective systems is favored. On the other hand, if the thermal equator deviates from the equator, as is the case in the western Pacific during boreal summer, moisture supply to equatorial trapped waves is reduced and development along the equator abates. This suggests that equatorial wave activity is also an important factor determining the variability of SCA.

b. The 30–60-day convection seesaw

As documented in the previous subsection, the SCAs concentrate in the tropical Indian and western Pacific oceans, in particular during boreal summer. The 30–60-day variations of convection in these two regions not only have large amplitude, but also are nearly out of phase (Fig. 2). When the equatorial Indian Ocean undergoes an active period of convection, the tropical western Pacific often experiences an abnormal dry condition; whereas when convection increases over the

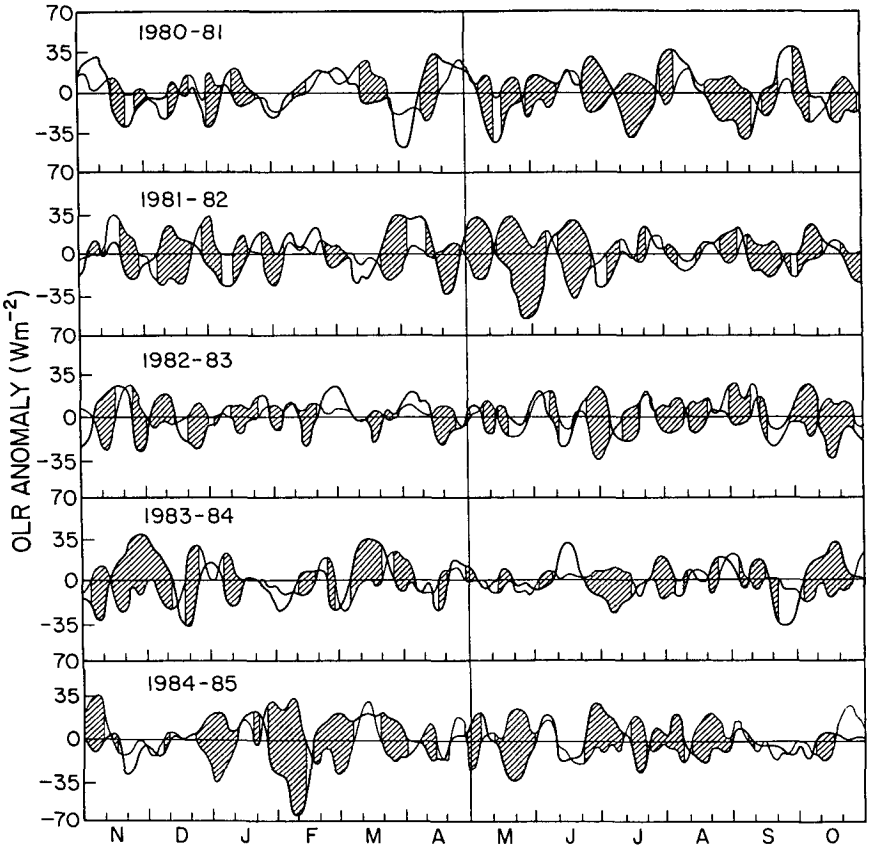

FIG. 2. Five-day running means of daily anomaly (annual and interannual variations filtered out) OLR series averaged over a 25° longitude and 15° latitude rectangular area in the equatorial Indian ocean centered at (0°, 82.5°E) (the thick lines) and in the equatorial western Pacific centered at (0°, 147.5°E) (the thin lines), respectively. The shading indicates the intervals during which the OLR anomalies in the two regions have opposite polarity.

western Pacific, the convection in the Indian Ocean is normally suppressed. The out-of-phase convective variation between the tropical Indian Ocean and western Pacific forms a standing oscillation with a nodal point over the maritime continent. We refer to this phenomenon as the 30–60-day convection seesaw between the tropical Indian and western Pacific oceans (hereafter referred to simply as convection seesaw).

It should be pointed out that the enhanced and suppressed convection over the western Pacific is not centered on the equator all year around; rather, it is concentrated over the Philippine Sea in boreal summer and over the SPCZ in boreal winter (Fig. 1). In addition, seesaw occurrence has significant interannual variation. For example, in the period 1975–1985, regular and persistent seesaws are seen in 1976, 1979, 1981, 1982, and 1985, while irregular and intermittent convection seesaws occur in 1980, 1983, and 1984 (figures for 1975–September 1980 are not shown). In 1976, the correlation coefficient of the OLR daily anomaly between the equatorial Indian and western Pacific oceans reaches an extreme value of −0.76.

4. Formation processes of the convection seesaw

a. Seesaw events and low-frequency convective systems

A seesaw event consists of two phases. The first phase is characterized by convection enhancement over the Indian Ocean and contemporaneous suppression of convection over the tropical western Pacific. The second phase is a subsequent reversal of locations of the enhanced and suppressed convection between the two pole regions. The entire event lasts at least six pentads.

Our working hypothesis is that the 30–60-day seesaw is a result of quasi-periodic recurrence of the development and movement of low-frequency convective systems (LFCSs). The two phases may either involve a single LFCS shifting from one pole to another or involve two separate LFCSs evolving at each of the poles and at each of the phases. We therefore will focus on the analysis of the interrelationship between the evolution of LFCS and seesaw.

In order to avoid subjectivity and vagueness in the analysis, we define an LFCS as a convection anomaly

that lasts at least four consecutive pentads and has a central OLR value below -25 W m^{-2} at its strongest stage. A large LFCS may last longer than 10 pentads and have a zonal dimension in excess of 100° longitude. The circulation anomalies associated with LFCS are primarily of planetary zonal scale (Weickmann et al. 1985). The LFCS defined here is essentially the same as the tropical intraseasonal convection anomaly defined previously by Wang and Rui (1990a).

Thirty-eight events were identified based upon the above considerations from five boreal winters (November–April) and summers (May–October). The central trajectories for each individual LFCS were plotted (not shown). In order to give a concise and informative description, time–longitude distribution of each LFCS center for all events is illustrated in Fig. 3. Also given is the information about the meridional displacement that exceeds 5° latitude per pentad. The strongest stages of the first and second phases defined above are selected according to the intensity and extent of the enhanced convection and associated suppressed convection. In reality, the two-dimensional trajectory is more complex than what is seen from the longitude–time diagram. Sometimes, one route may split into two subroutes; we trace only the principal one. In a few cases we also take the mean longitude of two splitting centers following the principle of historical continuity. Figure 3 is used to illustrate the synoptic processes of seesaw formation, which can be classified into two major categories that are principally season dependent.

b. *Boreal winter type*

A typical boreal winter event is associated with an eastward-traveling LFCS (Fig. 3). The system can be frequently traced back to Africa, but the amplitude there is small and the location is scattered. Its rapid development normally takes place over the equatorial Indian Ocean, followed by a weakening or splitting upon passing over the maritime continent. It often redevelops over the tropical western/central Pacific and finally decays in the eastern Pacific (Fig. 3). The above characteristic life cycle has been suggested by Rui and Wang (1990) based on a composite of 36 events. In a case study, Weickmann and Khalsa (1990) noticed that the shift of the convection anomaly from Indian Ocean to the western Pacific is rather swift. In Fig. 5 of Lau and Chan (1985), however, a fully developed anomaly is found over the maritime continent at day (0). This is probably an artifact of the one-point correlation map analysis in which the area-averaged OLR at Indonesia was chosen as a reference point for the correlation analysis.

Figures 4a and 4b show the convection seesaw patterns in boreal winter. The first phase of seesaw is marked by the most enhanced convection over the tropical Indian Ocean and the corresponding strongest suppressed convection scattering over the broad region of tropical western/central Pacific elongated more or less from northwest to southeast (Fig. 4a). The second phase of seesaw has enhanced convection over the SPCZ and suppressed convection over the Indian Ocean, forming an east–west dipole pattern slightly south of the equator (Fig. 4b). The first phase leads the second phase by about 15–25 days. Figures 4a and 4b suggest that the equatorial Indian Ocean and the SPCZ are action centers where 30–60-day convective anomalies undergo strong development or decay so that both the enhanced and suppressed convection tend to reach maxima there. We note that the LFCSs have a characteristic zonal scale of wavenumber 2. Their half wavelength matches well the distance between the central Indian Ocean and western Pacific. When these systems move eastward along the equator, a dipole pattern with opposite polarity is expected to emerge between these two regions. As a result, the enhanced and suppressed convection is phase-locked with the two action centers.

In summary, there are two factors that are crucial to the formation of the boreal winter seesaw. One is the weakening and/or splitting of the LFCSs near the Maritime Continent. The other is the out-of-phase enhancement between the tropical Indian Ocean and western Pacific. Both factors are linked to the characteristic life cycle and zonal scale of the eastward-propagating LFCSs. Because of this longitudinal intensity dependence, the collective behavior of many individual eastward-moving events contributes to the formation of the boreal winter seesaw.

In previous EOF or correlation map analysis (e.g., Lau and Chan 1985), the Madden–Julian mode was described as an east–west-oriented, fixed enhanced–suppressed convection dipole moving eastward. It is important to point out that this is not the case as described here for the winter seesaw. In the first phase of seesaw, the strong suppressed convection center occurs over the tropical western Pacific—that is, east (or ahead) of the enhanced convection center over the Indian Ocean. In the second phase, however, the original suppressed convection center ahead of the enhanced convection rapidly weakens and a new major suppressed convection center develops at the tropical Indian Ocean—that is, west (or behind) of the enhanced center. This indicates that the evolution of the eastward-propagating LFCS is strongly regulated by the two action centers, which contributes to the winter seesaw formation.

c. *Boreal summer type*

In contrast to the boreal winter seesaw, Fig. 3 indicates two distinct features of the LFCS activity during boreal summer: 1) Most seesaw events involve two LFCSs, a western system over the Indian Ocean and an eastern system over the tropical western Pacific, and

2) the two systems have short longitudinal displacements but often have significant meridional ones.

The majority of the western systems originate over the equatorial Indian Ocean. In about one-half of the cases the western system has significant eastward displacement (longer than 40° longitude); meanwhile, it turns northward or northeastward and disappears over the south Asian continent. Examples are cases 8011, 8105, and 8109, etc. (Fig. 3). This type of system (type 1) appears to arise from an equatorial Madden–Julian mode that is affected by monsoonal circulation at its later stage. Another half of the cases exhibit a major northward propagation without systematic and significant zonal propagation. There is an evident enhancement of convection during their northward journeys. The convection anomalies disappear finally over the Indian subcontinent or Southeast Asia. Such examples are cases 8107, 8207, 8208, and 8209, etc. (Fig. 3). This type of system (type 2) actively interplays with the Indian monsoons and is not rooted in the eastward-propagating equatorial mode. It is evident that the 40-day oscillation over the Indian summer monsoon region may be considered a result of the combined activities of the type 1 and type 2 systems.

It is interesting to notice that the type 2 systems occurred repetitively (five times) in 1982 from March to November, during which an exceptionally strong Pacific warming developed in the western and central Pacific. On the other hand, type 1 systems prevailed in 1979 (figure not shown). The latter was noticed by Krishnamurti et al. (1985) and Murakami and Nakazawa (1985). Considerable interannual variation regarding the nature of the western-system activity is thus implied.

It should be emphasized that the western system is only one component of the planetary-scale 30–60-day convection seesaw event. The other complementary component is an eastern system. Most eastern systems originate over the western North Pacific, gradually develop and migrate northward, and finally decay over the seaboard of eastern China or south of Japan (e.g., cases 8105, 8406, 8407, and 8505). In some cases (about one-third), the eastern systems can be traced back to the central Pacific, from where they migrate westward and turn northward when approaching the Philippines (e.g., case 8011, 8207, 8309, and 8410). The westward-propagating systems are usually weak but often intensify when turning northward. These two types of eastern systems were labeled as independent, northward-moving and westward-moving LFCSs, respectively, by Wang and Rui (1990a).

During boreal summer, the out-of-phase relationship between the enhanced and suppressed convection between the tropical Indian and western Pacific oceans is prominent. When the mature stages of the western systems occur over or north of the equatorial Indian Ocean (the first phase of seesaw), the suppressed convection centers are located in the region from the Philippine Sea to the south China Sea (Fig. 5a). This confirms Lau and Chan's (1986) previous finding using correlation maps. Figure 5b illustrates the seesaw pattern for the second phase during which the eastern systems reach their strongest stages. It is evident that a phase reversal occurs between the northern Indian Ocean and western Pacific monsoon trough regions. The development of the western system in general precedes that of its eastern counterpart by about 15–25 days. The aforementioned large-scale processes of the seesaw formation in boreal summer are very different from those in boreal winter.

In addition to the above two major categories of seesaw events, we also observed two special events in which the strongest development of convection anomalies over the western Pacific leads that over the Indian Ocean. One took place during October 1981 (Fig. 3). This special event consists of two independent northward-moving systems, but the development of the eastern system over the tropical western Pacific precedes that over the Indian Ocean as opposed to the regular boreal summer type. The other special case occurred in April 1984. The LFCS in this event first moved westward from the tropical central Pacific, weakened over the maritime continent and redeveloped in the Indian Ocean, followed by a northward turn over the northern Indian Ocean, and finally an eastward turn in subtropics. The presence of these singular events indicates the irregular nature of the seesaw.

We note also that during transitional seasons (late spring and fall) the seesaw events either fall into the boreal winter or boreal summer type. In May, normally boreal summer-type seesaw starts to occur (e.g., 1981, 1984, and 1985), but in certain years boreal winter-type seesaw remains dominant (e.g., 1982 and 1983). On the other hand, in November, boreal winter-type seesaw appears more frequently (e.g., 1981, 1983, and 1984), yet in some years it may be interrupted by late occurrence of the boreal summer-type seesaw (e.g., 1980 and 1982). There is no special seesaw event that is unique to the transitional seasons.

d. Recurrence of the seesaw event

The boreal winter- (summer-) type seesaw does not always occur during boreal winter (summer). In fact, among 19 boreal winter-type seesaw events, 3 occurred in boreal summer; similarly, 4 out of 17 boreal summer-type events occurred in boreal winter (Fig. 3).

Regardless of the complexity due to the alternative occurrence of the two types of events, the quasi-periodic recurrence of the seesaw is one of the outstanding features in Fig. 3. The average interval between two successive seesaw events is about 48 days. There are no evident seasonal changes of the oscillation period, which agrees with the results of the previous studies by Anderson et al. (1984) and Madden (1986).

The time interval between the first and second phases

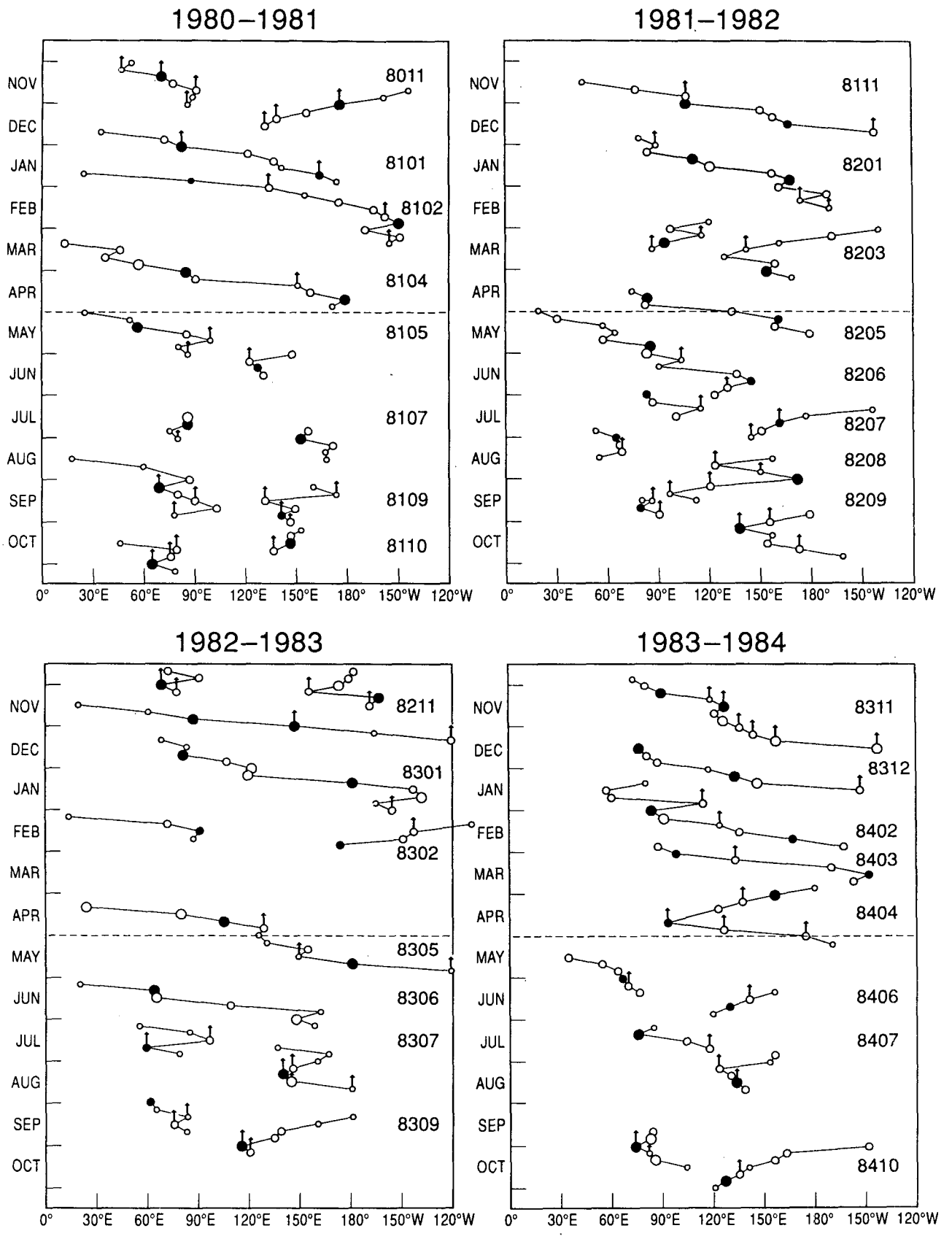
1980–1981
NOV
DEC
JAN
FEB
MAR
APR
MAY
JUN
JUL
AUG
SEP
OCT
8011
8101
8102
8104
8105
8107
8109
8110
0° 30°E 60°E 90°E 120°E 150°E 180° 150°W 120°W
1981–1982
8111
8201
8203
8205
8206
8207
8208
8209
1982–1983
8211
8301
8302
8305
8306
8307
8309
1983–1984
8311
8312
8402
8403
8404
8406
8407
8410

FIG. 3.

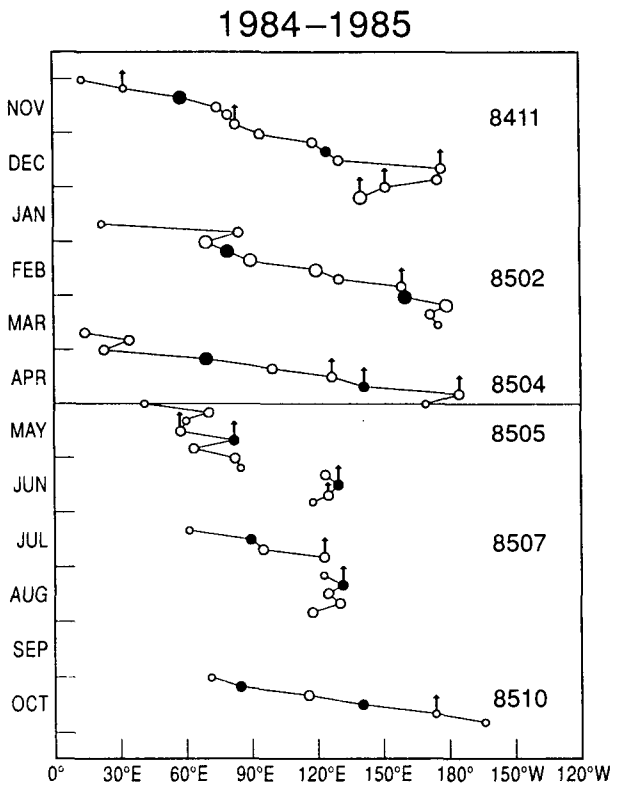

FIG. 3. The longitude–time diagram of the central tracks of low-frequency convective systems that are projected to the equator for November 1980–October 1985. The small, medium, and large sizes of the open and closed circles represent the minimum OLR anomalies between −15 and −25, between −25 and −35, and lower than −35 W m^{-2}, respectively. The strongest stages of the first and second phases of seesaw are marked by closed circles. The arrows are attached to indicate the northward movement with a total meridional displacement exceeding 5° latitude per pentad.

of seesaw varies from 15 to 25 days with an average of 20 days for all seasons. This is consistent with Lau and Chan's (1985, 1986) correlation map analysis, which showed that a phase reversal of the seesaw pattern occurs in about 20 days. The transition period between two phases (20 days) is shorter than the time interval for rebuilding a new seesaw pattern, which takes about 28 days. This temporal asymmetry, as will be seen in the case analyses (section 5), occurs because the rebuilding of a new seesaw is associated with a wavenumber 1 divergent circulation anomaly that takes about two excess pentads to traverse the western hemisphere.

5. Interrelation between convection seesaws and summer monsoons

In this section, two individual cases are presented in order to show specific examples of the statistical analysis in the previous section and to further elaborate on the relationship between convection seesaws and summer monsoon circulations.

a. A boreal winter case

The seesaw event of January–March 1985 is one of the most prominent winter 30–60-day oscillation events. It is depicted by two map sequences of pentad mean anomalies of OLR and 200-mb velocity potential shown on Figs. 6a and 6b, respectively. The seesaw event is due to an eastward-moving low-frequency convective system.

In the beginning of the event, several weak convection anomalies were scattered over the equatorial Africa and the western Indian Ocean. At pentad 3 (hereafter denoted as P-3) convection rapidly flared up over the Indian Ocean. The major convection anomaly further enhanced and expanded, reaching maximum strength at P-5 (Fig. 6a). When passing over the maritime continent–northern Australia region, the convection anomaly weakened and finally at P-7 broke down to two systems located to the east and west of Australia, respectively. The weakening and splitting processes are also reflected in velocity potential field (Fig. 6b). Soon after passing over the maritime continent–northern Australia, both the upper-level divergent circulation and convection anomalies immediately redeveloped over the SPCZ and extended into the eastern Pacific (P-9, Figs. 6a and 6b).

The first phase of seesaw (from P-3 to P-6) is attributed to sustained development of convection and associated low-level westerlies over the Indian Ocean, and to the suppressed convection and associated low-level easterly anomalies over the tropical western-central Pacific (Figs. 6a and 7). The equatorial westerly anomalies at the first phase of seesaw further extend eastward from P-6 to P-7, enhancing the summer monsoon westerlies over Indonesia and northern Australia. This suggests a close tie between the active Indonesia–Australia summer monsoon and the downstream development of the equatorial westerlies at the first phase of the seesaw. Holland (1986) showed that the Australian monsoon typically consists of 2–3 cycles of heavy rain, each lasting more than 2 pentads, followed by a somewhat longer break. The average period from peak-to-peak activity is around 40 days. Most of the active-break Australian summer monsoon cycles are closely related to the boreal winter seesaw events shown in Fig. 3. For instance, the early Australian summer monsoon onset (ASMO) occurred in December for 1981–82 and 1984–85, while late ASMO occurred in January for 1980–81 and 1982–83 (Joseph et al. 1991). Inspection of Fig. 3 reveals that the seesaw events 8111 and 8411, which are the earliest boreal winter-type seesaws of the corresponding seasons, contribute to the early ASMO, whereas the seesaw events 8101 and 8301 are linked to the late ASMO. Both the late ASMO were preceded by late occurrence of boreal

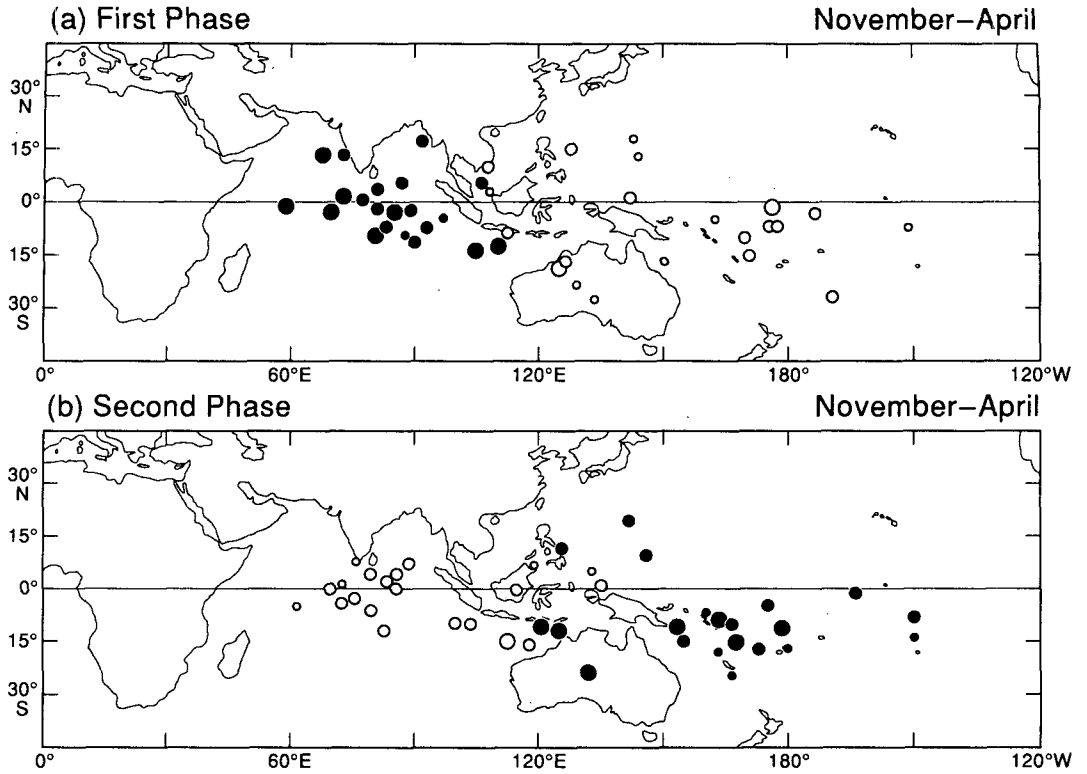

FIG. 4. Distribution of the central locations of the simultaneously enhanced (closed circle) and suppressed (open circle) convection at the strongest stages of the (a) first and (b) second phases of seesaw in the November–April season. The small, medium, and large sizes of the closed and open circles denote absolute values of anomalous OLR between 25 and 35, 35 and 45 W m^{-2}, and greater than 45 W m^{-2}, respectively.

summer-type seesaws in preceding October and November (case 8011 and 8211). The ASMO date in 1983–84 were confused by an early occurrence of monsoon westerlies in late November (but rainfall was slightly short of 7.5 mm day^{-1}) and a delayed occurrence of heavy rainfall in early January (Fig. 9 of Joseph et al. 1991). Figure 3 indicates that the late November onset of monsoon westerlies and the early January onset of monsoon rainfall are, respectively, associated with the seesaw events 8311 and 8312. In the former case, the convection anomaly persistently shifted northward, causing the deficient rainfall in the Australian monsoon region. The close association between the Australian monsoon activity and the 40–50-day oscillation was noticed previously by Murakami et al. (1986) and Hendon and Liebmann (1990).

The second phase of seesaw (P-8 to P-11) is mainly attributed to the redevelopment of convection and associated low-level westerlies over the western Pacific (Figs. 6a and 7a), which can be regarded as an active period of SPCZ summer monsoon. At this phase in the Indian Ocean, anomalous low-level easterlies prevail and the monsoons over Indonesia and northern Australia appear to experience a break (Fig. 7). An interesting feature of the redevelopment is that both the upper-level divergent circulation and convection anomalies change to a northwest–southeast orientation along the SPCZ. In fact, most of the enhanced convection over the western Pacific during the Austral summer displays a similar diagonal shape, resembling the mean state of SPCZ shown by Vincent (1982). This indicates that the circulation anomalies of the second phase of seesaw are strongly modified by the SPCZ disturbances and quite different from the first phase of seesaw.

b. A boreal summer case

The case of September–October 1984 is illustrated in Fig. 8 in terms of sequences of pentad mean anomaly maps of OLR and 200-mb velocity potential. The seesaw event was associated with the last spell of the Indian summer monsoon. It comprised a northward-moving LFCS over the Indian Ocean (the western system) at early stages (P-1 to P-5) and a northwestward-moving LFCS over the western Pacific (the eastern system) at later stages (P-5 to P-9) of the event. The strongest stage of the eastern system (P-7) lagged that of the western counterpart (P-3) by about 20 days. The convection seesaw was produced by the successive development of the western and the eastern systems.

The western system of the seesaw is a major player

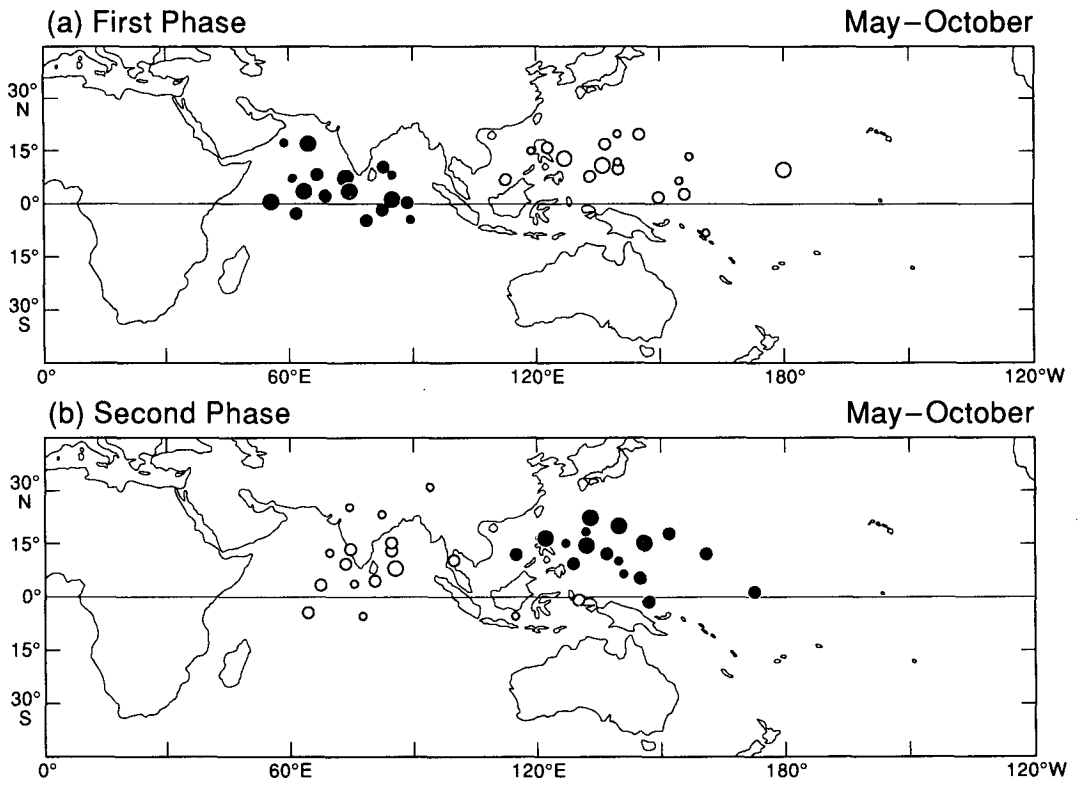

FIG. 5. As in Fig. 4 except for May–October season.

affecting the Indian monsoon. At the beginning of the event (P-1 and P-2), the 850-mb easterly anomalies prevailed over the Indian subcontinent (Fig. 9), whereas a convection anomaly developed over the central Indian Ocean within an equatorial trough. This marks a break of the Indian monsoon. At P-3, strong anomalous westerlies developed in the equatorial Indian Ocean and convection concurrently intensified with an anomalous cyclone near the south tip of the Indian subcontinent, establishing the first phase of seesaw (Figs. 8 and 9). From P-4 to P-6 the westerly and convection anomalies continuously progressed northward, affecting the weather in India, the Bay of Bengal, and Southeast Asia. This corresponds to an active monsoon period. By P-7, the 850-mb winds over the equatorial Indian Ocean reversed their direction in response to outburst of a strong cold surge from East China to South China Sea (Fig. 9), completing seasonal withdrawal of the Indian summer monsoon. The scenario documented here is an example of the association of a northward-propagating 40-day oscillation system with major active-break cycles of Indian monsoon, which was previously found and documented by Yasunari (1979, 1981), Krishnamurti and Subrahmanyam (1982), Murakami and Nakazawa (1985), and others.

In harmony with the reversal of polarity in convection seesaws, the western Pacific monsoon activity tends to be out-of-phase with the Indian monsoon: it is suppressed (enhanced) during the active (break) Indian monsoon at the first (second) phase of seesaw. A similar phenomenon is the out-of-phase relation between the Indian and east Asian summer monsoons described by Tao and Chen (1987). When anomalous westerlies shifted northward over the northern Indian Ocean from P-4 to P-5, the easterlies previously existing over the northwestern tropical Pacific were replaced by westerlies. At the time the westerlies rapidly abated over the Indian sector from P-6 to P-7, the westerlies over the western Pacific rapidly intensified (Fig. 9), establishing the second phase of seesaw. The strongest westerlies are tied with the enhanced northeasterlies from eastern Asia. During the transitional period of the East Asia monsoon, the activity of the northwestern Pacific monsoon trough is often enhanced due to the increased convergence between cold northeast winds and near-equatorial westerlies.

6. Summary

Previous studies have emphasized essential roles of the global-scale, eastward-propagating waves, the Madden–Julian (1972) mode, in the tropical 30–60-day oscillation. The present paper shows that the tropical 30–60-day oscillation exhibits a pronounced regional standing oscillation pattern in convection

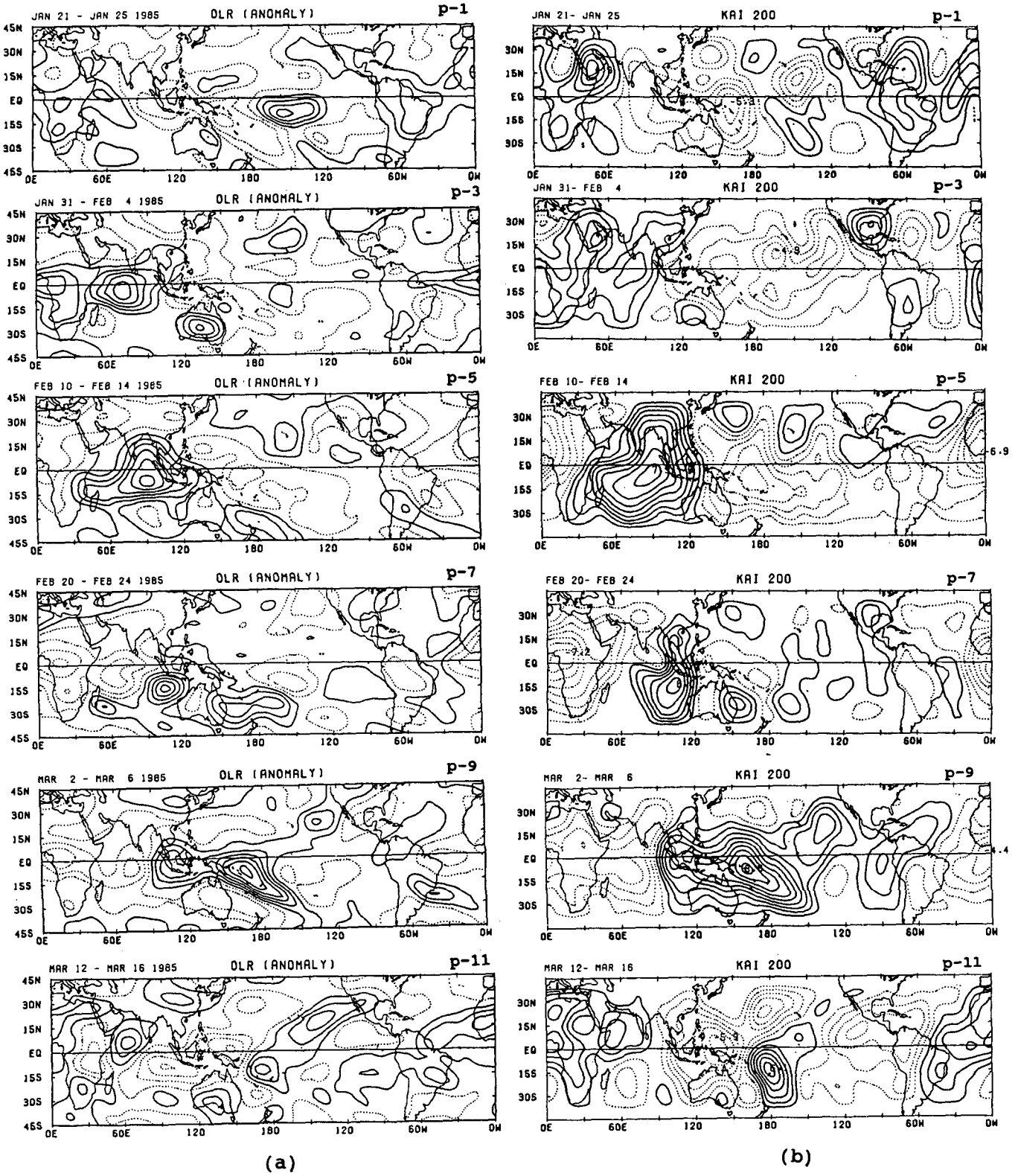

FIG. 6. (a) A sequence of pentad mean OLR anomaly maps for the case of 21 January–21 March 1985. P-1 to P-11 denote the first to the eleventh pentad during this period. Note that the solid (dotted) contours denote negative (positive) OLR. The contour interval is 10 W m^{-2}, and the lowest value of the positive contour is 5 W m^{-2}. (b) As in (a) except for 200-mb potential velocity field. The contour interval is 2×10^{-6} m^2 s^{-1}, and the first solid (dotted) curve starts from 10^{-6} (-10^{-6}) m^2 s^{-1}.

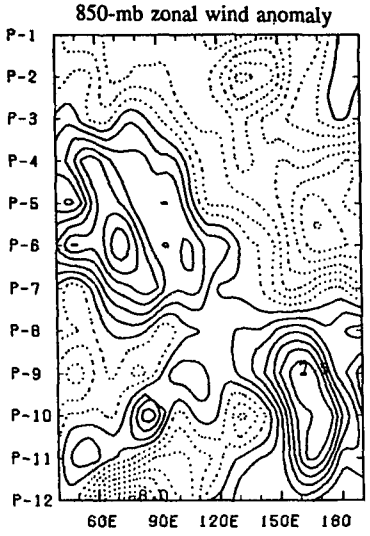

FIG. 7. Longitude–time diagram of 850-mb pentad mean anomalies of zonal wind averaged between the equator and 5°S. The contour interval is 1 m s^{-1}, and the first solid (dotted) contour denotes 0.5 (−0.5) m s^{-1}.

anomalies in addition to the propagating-wave character. One pole of the seesaw is the tropical Indian Ocean, and the other is the tropical western Pacific. The two polar regions of the convection seesaw are action centers for the 30–60-day oscillation, where the largest variabilities in both convection and circulation are observed (Figs. 1 and 2). Prominent northward (e.g., Yasunari 1980) and westward (e.g., Wang and Rui 1990a) propagation adds another unique feature to these regions. In sharp contrast, the smallest variability occurs over the Maritime Continent, which is the nodal point of the seesaw (Figs. 4 and 5).

There are two phases for each seesaw event. The first phase is characterized by a strongly developed convection over the equatorial Indian Ocean and concurrent suppressed convection over the tropical Pacific. The second phase displays a reversed polarity between the two poles of the seesaw. Both phases are in close connection with a global, eastward-propagating divergent wave. The formation process of the seesaw, however, is strikingly season dependent. The two synoptic models of seesaw formation proposed in section 4 are, respectively, typical for boreal winter and summer.

As a summary, we present in Fig. 10 a schematic depiction of the large-scale processes of the 30–60-day oscillation. The plotted zonal circulation cells refer to the divergent component of wind anomalies. Total wind anomalies are dominated by the rotational component even in the equatorial regions, and these are nearly in phase with the corresponding convection anomalies (e.g., Murakami 1988; Rui and Wang 1990). The convection and upper-level divergence anomalies are averaged for the equatorial belt between 15°N and 15°S, which are derived on the basis of the OLR and 200-mb velocity potential anomalies computed for the selected boreal winter and summer cases discussed in section 5.

The boreal winter model is a modification to Madden and Julian's (1972) schematic model of an eastward-moving circulation cell in the equatorial zonal plane. Their model was inferred from spectral analysis of winds and was conceptually an analogue to the anomalous Walker circulation in the Southern Oscillation as advanced by Bjerknes (1969). The principal modification in the present model (Fig. 10a) emphasizes longitudinal dependence of the life cycle of the propagating LFCSs: they strongly grow over the equatorial Indian Ocean, weaken or split over the maritime continent, and redevelop over the SPCZ. It is the collective behavior of the longitude-dependent evolution of eastward-moving LFCSs that is responsible for the formation of the boreal winter seesaw.

The boreal summer model reflects the fact that the seesaw formation involves two separate systems. The western system over the Indian Ocean either directly moves northward or initially moves eastward, followed by a northward turning, both interacting with the Indian monsoon. The eastern system over the western Pacific often originates in situ or in the central Pacific and drifts northward or propagates first westward then turns northward over the ocean east of the Maritime Continent. The successive persistent developments of the two systems consolidate a boreal summer-type convection seesaw.

Figure 10 stresses standing (seesaw) character of the 30–60-day oscillation, which occurs all year around, but the formation processes are season dependent. Note, however, that the time intervals between two successive strongest stages of a seesaw, and between two seesaw events, are, respectively, 15–25 and 35–60 days without significant annual variation. Figure 10 also emphasizes that the seesaw is intimately associated with intrinsic LFCSs. The propagating LFCSs and convection seesaws should be regarded as two aspects of a unified phenomenon. Their coherent variations produce global as well as regional 30–60-day oscillations.

The propagating systems associated with the seesaw move largely eastward along the equator, especially during boreal winter and over the Indian Ocean. Their behavior resembles, to the first-order approximation, a moist Kelvin wave (Lau and Peng 1987; Chang and Lim 1988; Wang 1988) or, more precisely, a modified moist Kelvin wave coupled with long Rossby waves (Wang and Rui 1990b). Their characteristic zonal scales (a dominant wavenumber 1 circulation pattern and a much smaller convection scale of a few thousand kilometers) can be explained by the nonlinear heating effects (Lim et al. 1990; Wang and Xue 1992). During boreal summer, about a half of the western systems bear some resemblance to the moist equatorial Kelvin wave packet at early stage and experience northward

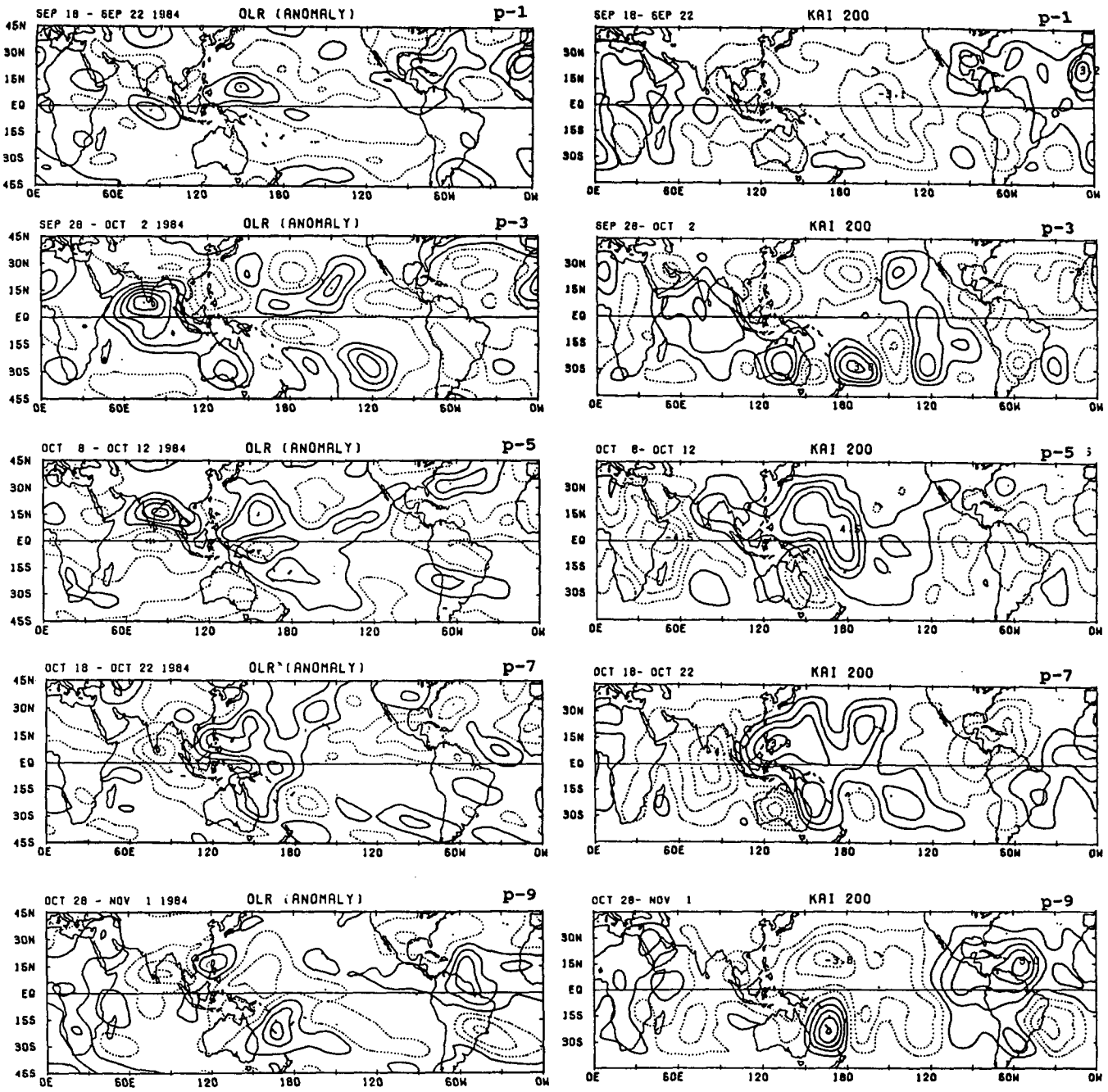

FIG. 8. As in Fig. 6 except for the event of September–October 1984.

deflection as they interact with the Indian summer monsoon. Another half of the western systems are locally northward-propagating divergent circulations, the nature of which is not well understood. Simple monsoon model analysis has suggested that the poleward propagation occurs in the presence of a meridional temperature gradient because the convective heating is asymmetric (Gadgil and Srinivasan 1990). On the other hand, Lau and Peng (1990) suggested that when the equatorial low-frequency mode interacts with monsoonal flow, a group of synoptic-scale disturbances may be excited along 15°N, which corresponds to a

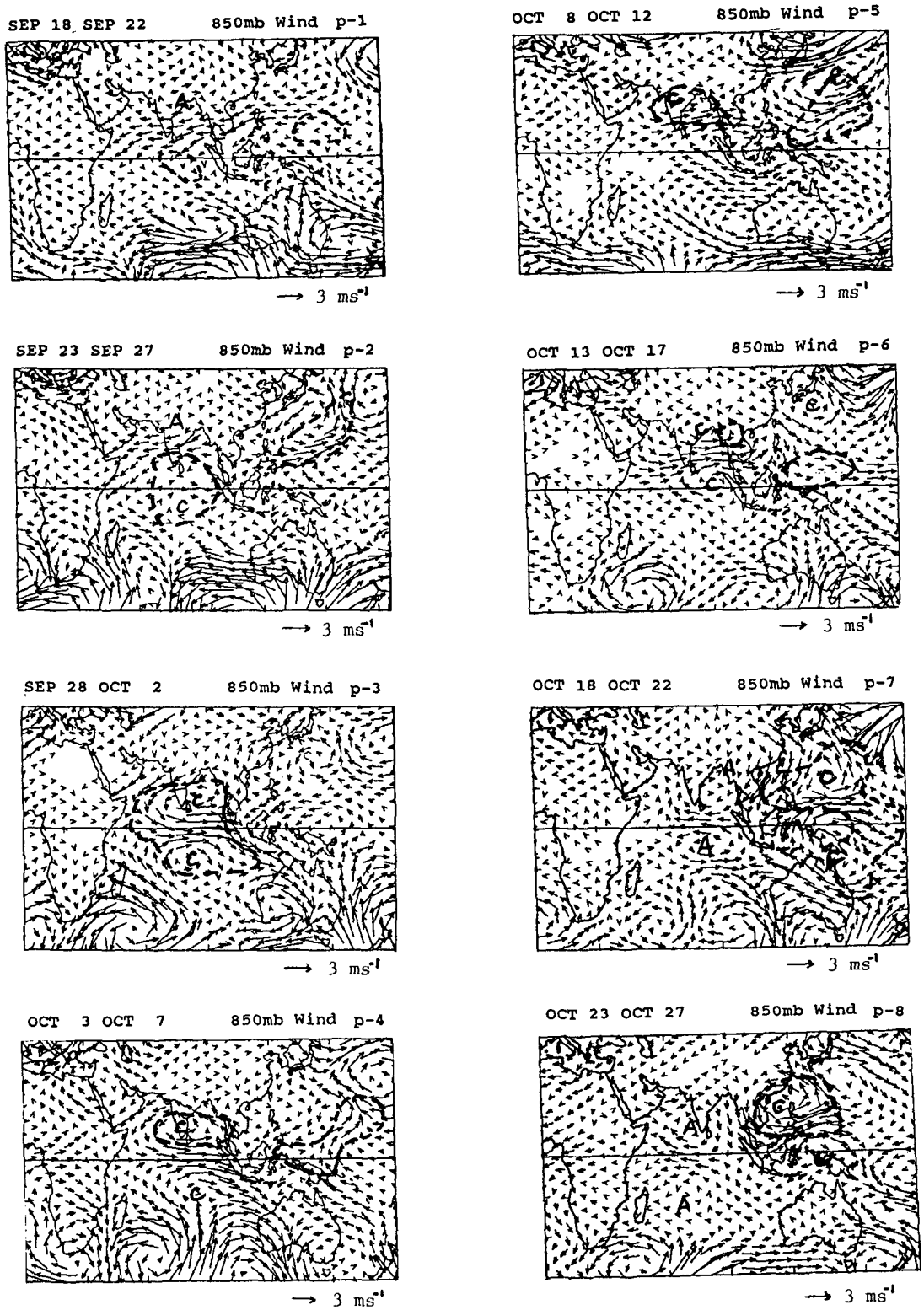

FIG. 9. Pentad mean anomaly maps of 850-mb wind for the pentads from P-1 (18–22 September) to P-8 (23–27 October 1984). The thick dashed lines denote locations of the major negative OLR anomalies. The letters "A" and "C" represent an anticyclone and cyclone, respectively.

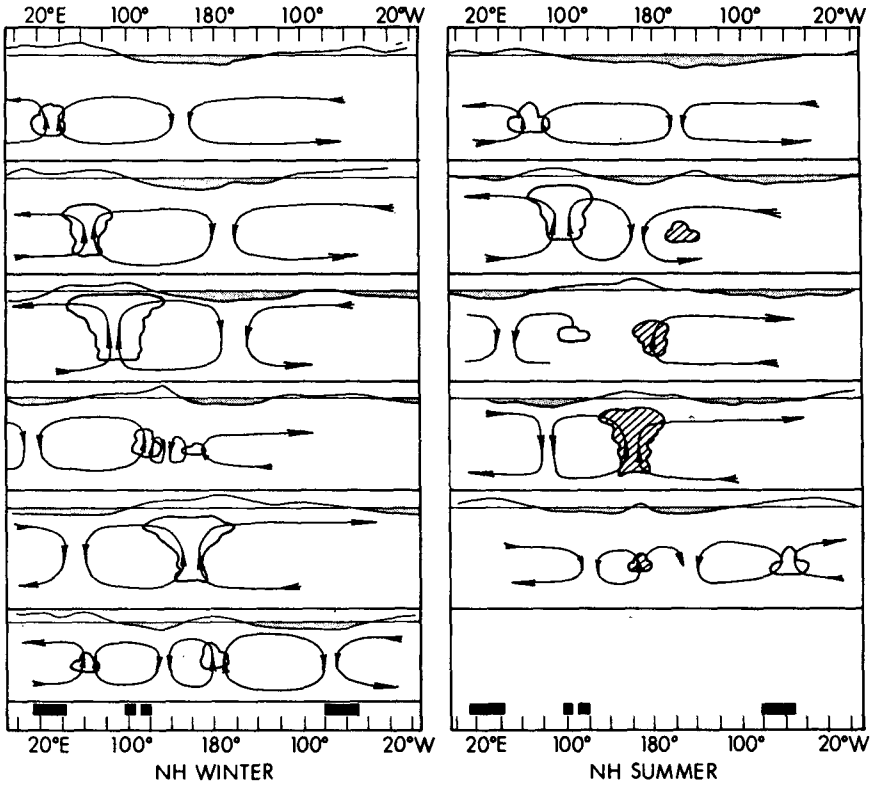

FIG. 10. Schematic models of the tropical 30–60-day oscillation projected onto the equatorial zonal plane for (a) boreal winter and (b) boreal summer. The curves above the convection anomalies are velocity potential anomalies at 200 mb with positive value denoting divergence. The plotted zonal wind represents the divergent component. For more explanations refer to the text.

sudden northward shift of the monsoon cloud band. The eastern system over the western Pacific, which consists of an off-equatorial rotational circulation anomaly, seems to be of the nature of a westward-propagating Rossby wave interacting with the monsoon circulation in situ.

Standing property of the seesaw is related to the preferred geographical regions where strong positive or negative 30–60-day convective anomalies persistently occur (the Indian Ocean near-equatorial trough, the SPCZ in boreal winter, and the northwest Pacific monsoon troughs in boreal summer). These regions are characterized by high SST (monthly mean SST higher than 28°C) and surface wind convergence. It is reasonable to conclude that warm oceanic convergence zones are favorable for the development of LFCS. In contrast, the Maritime Continent is geographically preferred for the weakening of many cases given in Fig. 3. The maintenance of dipole patterns of seesaw is ascribed to this geographic dependence of the development characteristics.

During boreal winter, the buildup of the first developing phase results from frequent development of moist Kelvin waves over the equatorial Indian Ocean, which often enhance Indonesian–Australian summer monsoons, while causing a break in the SPCZ and suppressing the convection in the SWICZ. During the second phase, the LFCSs interact with the monsoon circulation in the SPCZ. In boreal summer, the establishment of the first developing phase is related to the active period of the Indian monsoon with a break in the western Pacific monsoon, whereas the second phase is almost opposite.

In summary, the convection seesaw between the tropical Indian and western Pacific oceans is one of the fundamental characteristics of the tropical 30–60-day oscillation. The seesaw formation is in association with the interaction between propagating low-frequency systems and the summer monsoon circulations in both hemispheres. The Indian, western Pacific, Indonesian, Australian, and SPCZ monsoons are all semipermanent features of the tropical general circulation. They are strongly influenced by the land–sea thermal contrast, SST distribution, and mountains (Hahn and Manabe 1975; Kiladis et al. 1989; Wang and Li 1992, and others). The results raise a number of questions, of which the following are of particular interest:

- What are the dynamic effects of the ocean–continent thermal contrast, SST distribution, and monsoons on the preferred locations for LFCS that lead to the formation of a seesaw?
- What are the physical mechanisms responsible for the weakening or splitting of the LFCSs over the Maritime Continent?

These questions require further theoretical and numerical modeling studies.

Acknowledgments. The authors wish to thank Professor T. Murakami and anonymous reviewers for their valuable comments on early versions of the manuscript. Thanks are due Mr. Z. Tang and Ms. Diane Henderson for their graphical and technical assistance. This study was supported by the Climate Dynamics Division of NSF under the Grant ATM-9010315 and the EPOCS program of NOAA under Grant NA90RAH00074.

REFERENCES

Anderson, J. R., D. E. Stevens, and P. R. Julian, 1984: Temporal variations of the tropical 40–50 day oscillation. *Mon. Wea. Rev.*, **112,** 2431–2438.

Bjerknes, J., 1969: Atmospheric teleconnections from the equatorial Pacific. *Mon. Wea. Rev.*, **97,** 163–172.

Chang, C.-P., and H. Lim, 1988: Kelvin wave–CISK: A possible mechanism for the 30–50 day oscillation. *J. Atmos. Sci.*, **45,** 1709–1720.

Gadgil, S., and J. Srinivasan, 1990: Low frequency variation of tropical convergence zones. *Meteor. Atmos. Phys.*, **44,** 119–132.

Hahn, D. G., and S. Manabe, 1975: The role of mountains in the South Asian monsoon circulation. *J. Atmos. Sci.*, **32,** 1515–1541.

Hendon, H. H., and B. Liebmann, 1990: A composite study of onset of the Australia summer monsoon. *J. Atmos. Sci.*, **47,** 2227–2240.

Holland, G. J., 1986: Interannual variability of the Australian monsoon at Darwin: 1952–1982. *Mon. Wea. Rev.*, **114,** 594–604.

Joseph, P. V., B. Liebmann, and H. H. Hendon, 1991: Interannual variability of the Australia monsoon onset: Possible influence of Indian Summer monsoon and El Niño. *J. Climate,* **4,** 529–538.

Julian, P. R., and R. A. Madden, 1981: Comments on a paper by T. Yasunari, A quasi-stationary appearance of 30 to 40 day period in the cloudiness fluctuation during the summer monsoon over India. *J. Meteor. Soc. Japan,* **59,** 435–437.

Kiladis, G. N., H. von Storch, and H. van Loon, 1989: Origin of the South Pacific Convergence Zone. *J. Climate,* **2,** 1185–1195.

Knutson, T. R., and K. M. Weickmann, 1987: 30–60 day atmospheric oscillation: Composite life cycles of convection and circulation anomalies. *Mon. Wea. Rev.*, **115,** 1407–1436.

——, ——, and J. E. Kutzbach, 1986: Global-scale intraseasonal oscillation of outgoing longwave radiation and 200 mb zonal wind during Northern Hemisphere summer. *Mon. Wea. Rev.*, **114,** 605–623.

Krishnamurti, T. N., and D. Subrahmanyam, 1982: The 30–50 day mode at 850 mb during MONEX. *J. Atmos. Sci.*, **39,** 2088–2095.

——, P. K. Jayakumar, J. Sheng, N. Surgi, and A. Kumar, 1985: Divergent circulations on the 30–50 day time scale. *J. Atmos. Sci.*, **42,** 364–375.

Lau, K.-M., and P. H. Chan, 1985: Aspects of the 40–50 day oscillation during the northern winter as inferred from outgoing longwave radiation. *Mon. Wea. Rev.*, **113,** 1889–1909.

——, and ——, 1986: Aspects of the 40–50 day oscillation during the northern summer as inferred from outgoing longwave radiation. *Mon. Wea. Rev.*, **114,** 1354–1367.

——, and L. Peng, 1987: Origin of low frequency (intraseasonal) oscillation in the tropical atmosphere. *J. Atmos. Sci.*, **44,** 950–972.

——, and ——, 1990: Origin of the low frequency intraseasonal, oscillation in the tropical atmosphere. Part III: Monsoon dynamics. *J. Atmos. Sci.*, **47,** 1443–1462.

Lim, H., T.-K. Lim, and C.-P. Chang, 1990: Reexamination of wave–CISK theory: Existence and properties of non-linear wave–CISK modes. *J. Atmos. Sci.*, **47,** 3078–3091.

Lorenc, A. C., 1984: The evolution of planetary scale 200 mb divergent flow during the FGGE year. *Quart. J. Roy. Meteor. Soc.*, **110,** 427–441.

Madden, R. A., 1986: Seasonal variations of the 40–50 day oscillation in the tropics. *J. Atmos. Sci.*, **43,** 3138–3158.

——, and P. R. Julian, 1971: Detection of a 40–50 day oscillation in the zonal wind in the tropical Pacific. *J. Atmos. Sci.*, **28,** 702–708.

——, and ——, 1972: Description of global-scale circulation cells in the tropics with a 40–50 day period. *J. Atmos. Sci.*, **29,** 1109–1123.

Murakami, T., 1988: Intraseasonal atmospheric teleconnection patterns during the Northern Hemisphere winter. *J. Climate,* **1,** 117–131.

——, and T. Nakazawa, 1985: Tropical 45 day oscillations during the 1979 northern summer. *J. Atmos. Sci.*, **42,** 1107–1122.

——, L.-X. Chen, and A. Xie, 1986: Relationship among seasonal cycles, low-frequency oscillations, and transient disturbances as revealed from outgoing longwave radiation data. *Mon. Wea. Rev.*, **114,** 1456–1465.

Rui, H., and B. Wang, 1990: Development characteristics and dynamic structure of tropical intraseasonal convection anomalies. *J. Atmos. Sci.*, **47,** 357–379.

Tao, S., and L. Chen, 1987: A review of recent research on the east Asian summer monsoon in China. *Monsoon Meteorology,* C. P. Chang and T. N. Krishnamurti, Eds., Oxford, 60–92.

Vincent, D. G., 1982: Circulation features over the South Pacific during 10–18 January 1979. *Mon. Wea. Rev.*, **110,** 981–993.

Wang, B., 1988: Dynamics of tropical low-frequency waves: An analysis of the moist Kelvin wave. *J. Atmos. Sci.*, **45,** 2051–2065.

——, and H. Rui, 1990a: Synoptic climatology of transient tropical intraseasonal convection anomalies: 1975–1985. *Meteor. Atmos. Phys.*, **44,** 43–62.

——, and ——, 1990b: Dynamics of the coupled moist Kelvin–Rossby wave on an equatorial beta-plane. *J. Atmos. Sci.*, **47,** 397–413.

——, and T. Li, 1992: A simple tropical atmosphere model of relevance to short-term climate variations. *J. Atmos. Sci.*, in press.

——, and Y. Xue, 1992: On the behavior of a moist Kelvin wave packet with nonlinear heating. *J. Atmos. Sci.*, **49,** 549–559.

Weickmann, K. M., and S. J. S. Khalsa, 1990: The shift of convection from the Indian Ocean to the western Pacific Ocean during a 30–60 day oscillation. *Mon. Wea. Rev.*, **118,** 964–978.

——, G. R. Lusky, and J. E. Kutzbach, 1985: Intraseasonal (30–60 day) fluctuations of outgoing longwave radiation and 250 mb streamfunction during northern winter. *Mon. Wea. Rev.*, **113,** 941–960.

Yasunari, T., 1979: Cloudiness fluctuations associated with the Northern Hemisphere summer monsoon. *J. Meteor. Soc. Japan,* **57,** 227–242.

——, 1980: A quasi-stationary appearance of 30–40 day period in the cloudiness fluctuations during the summer monsoon over India. *J. Meteor. Soc. Japan,* **58,** 225–229.

——, 1981: Structure of an Indian summer monsoon system with a period around 40 days. *J. Meteor. Soc. Japan,* **59,** 336–354.